Polymeric multi-channel bandpass filters in phase-shifted Bragg waveguide gratings by direct electron beam writing

Lin Zhu, Yanyi Huang,* William M. J. Green, Amnon Yariv

Department of Electrical Engineering and Department of Applied Physics, California Institute of Technology
Pasadena, California 91125
yanyi@caltech.edu

Abstract: We apply direct electron beam writing to fabricate corrugated sidewall Bragg gratings in polymer waveguides and demonstrate multi-channel passband filters based on a phase-shifted design. Experimental results are compared with numerical fittings to analyze the impact of signal polarization and waveguide cladding material upon device performance.

OCIS codes: (350.2770) Gratings; (230.7390) Waveguides, Planar; (050.5080) Phase Shift

References and links

1. J.Canning, M.G.Sceats, "Phase-shifted periodic distributed structure in optical fibers by UV post processing," Electron. Lett. **30**, 1344-1345 (1994).
2. F.Bakhti, P.Sansonetti, "Design and realization of multiple quarter-wave phase-shifts UV-written bandpass filters in optical fibers," J. Lightwave Technol. **15**, 1433-1437 (1997).
3. K.Sugden, L.Zhang, J.A.R.Williamss, R.W.Fallon, L.A.Everall, L.A.Everall, K.E.Chisholm, "Fabrication and characterization of bandpass filters based on concatenated chirped fiber gratings," J. Lightwave Technol. **15**, 1424-1432 (1997).
4. R.C.Alferness, C.H.Joyner, M.D.Divino, M.J.R.Martyak, L.L.Buhl, "Narrowband grating resonator filters in InGaAsP/InP waveguides," Appl. Phys. Lett. **49**, 125-127 (1986).
5. W.C.Wang, M.Fisher, A.Yacoubian, J.Menders, "Phase-shifted Bragg grating filters in polymer waveguides," IEEE Photon. Technol. Lett. **15**, 548-550 (2003).
6. M.C.Oh, M.H.Lee, J.H.Ahn, H.J.Lee, S.G.Han, "Polymeric wavelength filters with polymer gratings," Appl. Phys. Lett. **72**, 1559-1561 (1998).
7. M.C.Oh, H.J.Lee, M.H.Lee, J.H.Ahn, S.G.Han, H.G.Kim "Tunable wavelength filters with Bragg gratings in polymer waveguides," Appl. Phys. Lett. **73**, 2543-2546 (1998).
8. L.Eldada, S.Yin, C.Poga, C.Glass, R.Blomquist, R.A.Norwood, "Integrated multichannel OADMs using polymer Bragg grating MZIs," IEEE Photon. Technol. Lett. **10**, 1416-1418 (1998).
9. T.Segawa, S.Matsuo, Y.Ohiso, T.Ishii, H.Suzuki, "Apodised sampled grating using InGaAsP/InP deep-ridge waveguide with vertical-groove surface grating," Electron. Lett. **40**, 804-805 (2004).
10. A.Yariv, P.Yeh, *Optical waves in crystals* (Wiley Interscience, 2003).

1. Introduction

In recent years, low cost bandpass filters have become key components for wavelength division multiplexing (WDM) metro networks. Optical transmission/reflection filters based on Bragg gratings have been widely investigated in photosensitive fibers [1-3], semiconductor waveguides [4] and polymer waveguides [5]. In order to reduce the system cost, bandpass transmission filters using phase shifts in Bragg gratings have been proposed since they can eliminate the need for a circulator. Meanwhile, planar polymeric waveguide devices, such as directional couplers, Mach-Zehnder interferometers, ring resonators, and Bragg grating reflectors, are becoming increasingly attractive for optical integrated circuits owing to the low cost and mechanical flexibility of polymer materials. Thus, it is very promising to incorporate

#5681 - $15.00 US Received 8 November 2004; revised 6 December 2004; accepted 6 December 2004

Bragg gratings with the multiple phase shift design within polymer waveguides for making low cost multi-channel bandpass filters.

Currently, polymeric Bragg grating filters are primarily fabricated by exposing the polymer with UV or visible light through a pre-designed phase mask [5-8]. Oh et al demonstrated wavelength filters based on uniform gratings in fluorinated polymer waveguides and successfully tuned them through the thermo-optic induced refractive index change [6,7]. Eldada et al wrote simple Bragg gratings in polymer waveguides to build multichannel optical add/drop multiplexers (OADM's) [8]. Wang reported the fabrication of a very narrow band phase-shifted Bragg grating filter, using a 457nm Ar^+ laser to post process the uniform waveguide gratings through the photobleaching effect [5]. However, it is diffucult to obtain a large index modulation using photobleaching. During the past two decades, electron beam lithography has been widely applied in fabricating complex micro/nano structures. In this paper, we apply direct electron beam writing to make corrugated sidewall Bragg gratings in polymer waveguides and demonstrate phase-shifted passband filters by introducing defects in the grating structure.

2. Grating design and fabrication process

Figure 1 shows schematic diagrams of the polymeric ridge waveguide with a corrugated sidewall Bragg grating and the corresponding effective refractive index profile along the propagation direction. In Fig. 1(a), the uniform gratings are formed by introducing periodic vertical grooves along the waveguide sidewall, which cause a periodic change in the refractive index of the waveguide. This design is superior to the conventional buried grating structure for the control of effective refractive index modulation, since a spatially varying index modulation profile may be engineered easily, by changing the grating groove depth [9]. By appropriately choosing the groove depth D, it is possible to achieve a significant relative refractive index modulation $\Delta n/n$ of ~0.001-0.1. The π phase shift required for a passband Bragg filter can be created by introducing a defect in the periodic structure, corresponding to a quarter wavelength discontinuity.

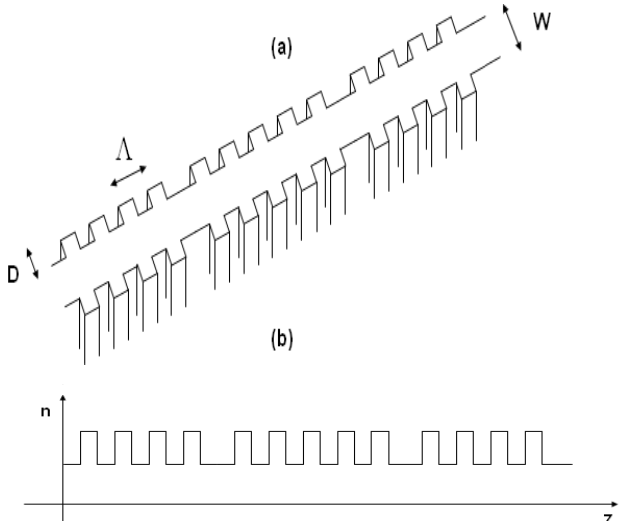

Fig. 1. Schematic diagrams of (a) polymeric waveguide gratings with two phase shift defects, and (b) the corresponding effective refractive index profile along the propagation direction.

To fabricate the device in Fig. 1(a), a 1.6 μm thick optical core layer of the negative electron beam resist SU-8 is first spun onto a silicon wafer with 5 μm of thermally grown silicon oxide, which serves as the lower cladding. Then, waveguides with corrugated sidewall gratings are directly patterned by electron beam exposure using a scanning electron microscope (SEM). As the waveguide core, the crosslinked SU-8 exhibits a relatively high

#5681 - $15.00 US Received 8 November 2004; revised 6 December 2004; accepted 6 December 2004

refractive index (n=1.565 at 1550nm) and low optical loss, making it an ideal polymeric optical material. Finally, the sample is developed by propylene glycol monomethyl ether acetate and dried by nitrogen gas. The waveguide end facets are formed by cleaving the silicon substrate. Figure 2 shows an SEM image of a completed device with a waveguide width W of 1.5 μm, grating period Λ of 500nm, and grating depth D of 600nm.

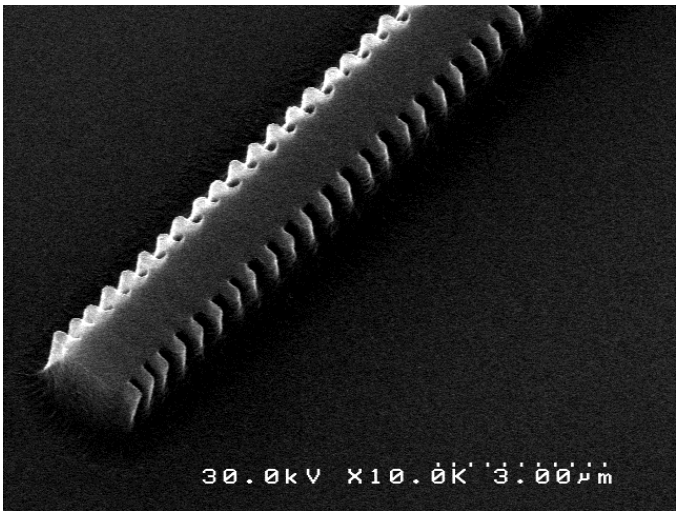

Fig. 2. SEM image of a polymeric grating device with a waveguide width W of 1.5 μm, grating period Λ of 500 nm, and grating depth D of 600 nm.

3. Experimental results and discussions

For measurement, a tunable laser provides transverse-electric (TE) or transverse-magnetic (TM) optical input signal through a paddle polarization controller. The light is coupled into one end of the device using a tapered fiber. The output optical signal, collected by an objective from the other end facet of the device, is measured by a femtowatt infrared photoreceiver. An oscilloscope is used to obtain the transmission spectrum of the device as the tunable laser scans the measurement wavelength.

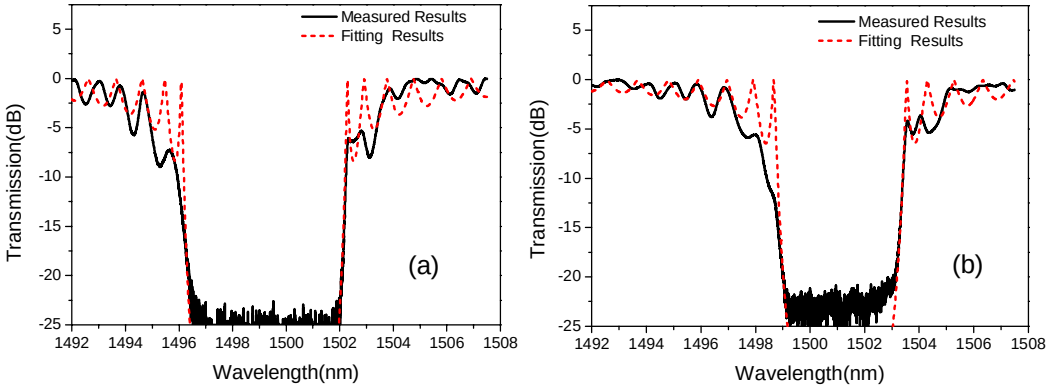

Fig. 3. Transmission spectrum of a uniform grating filter (a) TE polarization, n_{eff} = 1.4992 and Δn = 0.0090 from fitting results (b) TM polarization, n_{eff} = 1.5011 and Δn = 0.0067 from fitting results.

#5681 - $15.00 US Received 8 November 2004; revised 6 December 2004; accepted 6 December 2004

Figure 3 shows the transmission spectrum of a uniform grating filter for both TE and TM polarizations. The grating length is 630 μm. The device is generated with an electron exposure dosage of 10 μC/cm^2 and 7 pA writing current. The solid lines represent the experimental results and the dashed lines represent numerical fittings based on a transmission matrix method [10]. The combination of the tunable laser and the photoreceiver makes it possible to obtain a high resolution measurement of the grating spectral response, but the background noise floor limits the measured stopband rejection to about -25dB [2]. Correspondingly, the minimum relative transmission power level of the numerical calculation is set at around -25 dB to make a reasonable comparison between the experiment results and the theoretical fit.

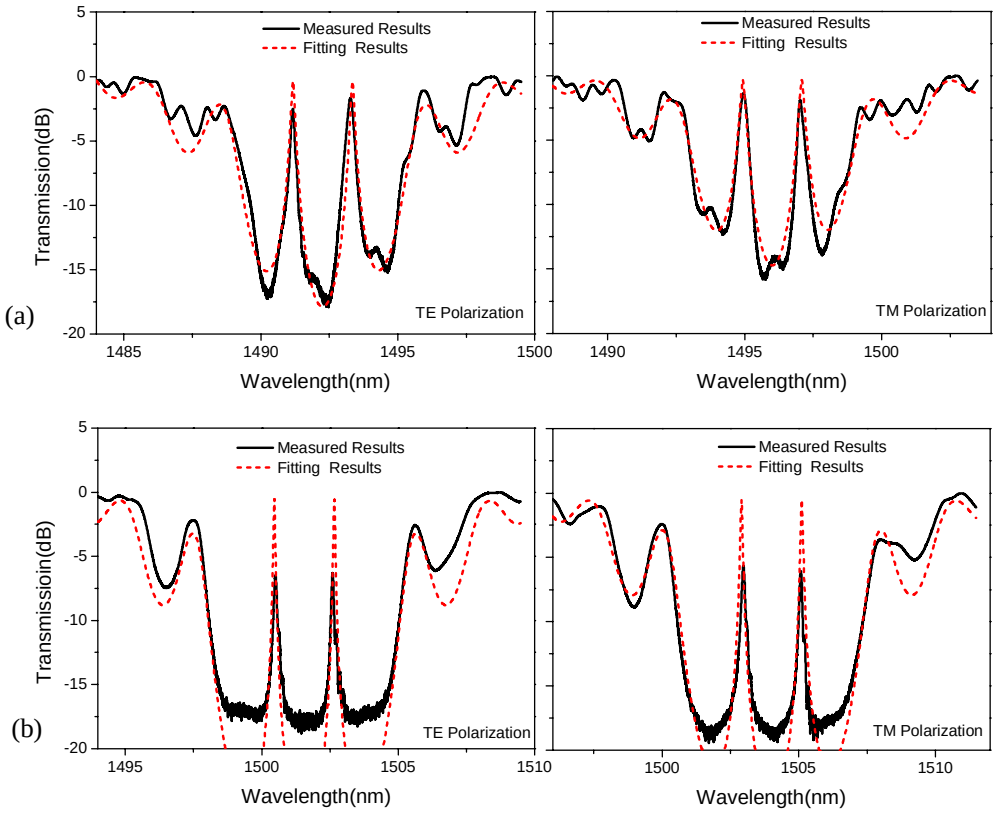

Fig. 4. Transmission spectrum of a passband filter with phase shift defects for TE polarization (a) without the index matching fluid, for TE polarization n_{eff} = 1.4923 and Δn = 0.0050 from fitting results, for TM polarization n_{eff} = 1.4960 and Δn = 0.0042 from fitting results (b) with the index matching fluid as upper cladding, for TE polarization n_{eff} = 1.5016 and Δn = 0.0070 from fitting results, for TM polarization n_{eff} = 1.5040 and Δn = 0.0064 from fitting results.

In Fig. 3(a), for TE polarization, the central wavelength is around 1.4992 μm, and the bandwidth is about 5.9nm with less than -20 dB transmission. According to the numerical fittings, the measured spectrum corresponds to a grating index modulation Δn of 0.0090. In Fig. 3(b), the central wavelength and bandwidth for TM polarization are 1.5001 μm and 4.2 nm (Δn = 0.0067), respectively. The higher effective index of the waveguide structure for TM polarization causes the red shift of the central wavelength. Because the gratings are designed along the sidewall, the TE polarization experiences a larger refractive index modulation,

#5681 - $15.00 US Received 8 November 2004; revised 6 December 2004; accepted 6 December 2004

which leads to the larger stopband bandwidth. In general, both TE and TM modes achieve a large stopband bandwidth, which is important for the design of multi-channel transmission filters incorporating multiple defect-induced phase shifts in the grating.

Figure 4 shows the spectral response of a multi-channel passband filter based on a polymer waveguide grating with two intentionally introduced π phase shifts. The device structure is very similar to that shown in Fig. 1(a). The defects are separated by a 90 μm segment of uniform grating, and the total length of the device is 720 μm. The tested device in Fig. 4 is generated under an electron exposure dosage of 10 $\mu C/cm^2$ with a current of 6.8 pA. In Fig. 4(a), the bandwidth of the stopband and the two passbands are 5.2 nm and 0.8 nm respectively for TE polarization, while being 5.4 nm and 0.8 nm for TM polarization. The spectra in Fig. 4(b) are obtained after applying a ~10 μm thick layer of index matching fluid (n = 1.44 at 1550 nm) over the top of the original device. It shows that the bandwidth of the stopband and the two passbands are 6.8 nm and 0.4 nm respectively for TE polarization, while being 6.7 nm and 0.4 nm for TM polarization. The band rejection level for both polarizations is about 11 dB. In Fig. 4(b), comparison of the experimental data with the fitting results shows that the measured transmission in the passband channels is lower than expected, and that the stopband minimum is higher. These discrepancies are attributed to scattering loss/fabrication errors and photodetector dark current/undesired laser scattering, respectively. In Fig. 4, the difference of central wavelength and bandwidth between TE polarization and TM polarization is consistent with the measurement results of the uniform waveguide grating in Fig. 3. By appropriately engineering the number and position of defects, it is possible to make flat-top channel filters, which are more suitable for the practical WDM system [2].

The index matching fluid serves two main functions. First, it eliminates reflections from the two cleaved end facets of the device, and the associated Fabry-Perot resonances, which can be clearly observed in Fig. 4(a). Second, it acts as an upper cladding material for the waveguide gratings. In Fig. 4(b), the central wavelength of the device is longer than in Fig. 4(a). This is because the additional upper cladding material causes the modal effective index to increase. We also find that the stopband is broader and the passband is sharper in the presence of index matching fluid. This is due to a larger effective refractive index modulation experienced by the cladded device in Fig. 4(b). The larger Δn is caused by the upper cladding fluid, since the optical mode is less confined after application. Thus, the groove features have a more significant impact on the mode in the waveguide. In fact, the use of upper cladding materials with different refractive indexes provides a simple but effective method to post tune the filter spectral response.

4. Conclusion

We successfully use electron beam direct writing to fabricate a multiple channel passband filter in a polymer waveguide with phase-shifted corrugated sidewall Bragg gratings. Two 0.4 nm passbands with an 11 dB rejection level are symmetrically embedded within a 6.8 nm stopband. We also analyze the impact of signal polarization and upper waveguide cladding on the performance of the designed filter.

Acknowledgments

The authors thank J. Choi, W. Liang, G. Paloczi, J. Poon, Dr. J. Scheuer, and Dr. Y. Xu for helpful discussions. Financial support from the National Science Foundation and Defense Advanced Research Projects Agency (Dr. D.Honey and Dr. R. Athale) is gratefully acknowledged.

#5681 - $15.00 US Received 8 November 2004; revised 6 December 2004; accepted 6 December 2004